TISSUE ENGINEERING: Part A
Volume 24, Numbers 21 and 22, 2018

DOI: 10.1089/ten.tea.2018.0013

termis
Tissue Engineering
& Regenerative Medicine
International Society

ORIGINAL ARTICLE

Sclerostin-Neutralizing Antibody Enhances Bone Regeneration Around Oral Implants

Shan Huey Yu, DDS, MS,[1] Jie Hao, MD,[1] Tobias Fretwurst, DDS, DMD,[1,2] Min Liu, PhD,[3] Paul Kostenuik, PhD,[1,3,6] William V. Giannobile, DDS, DMedSc,[1,4] and Qiming Jin, DDS, MS, PhD[5]

Background: Dental implants are an important option for replacement of missing teeth. A major clinical challenge is how best to accelerate bone regeneration and reduce the healing time for functional restoration after implant placement. A sclerostin-neutralizing antibody (Scl-Ab) has been shown to enhance alveolar bone formation and fracture repair. The aim of this study was to investigate the effects of systemic administration of Scl-Ab on dental implant osseointegration and bone regeneration in an experimental alveolar ridge tooth extraction model.
Materials and Methods: To investigate the effects of Scl-Ab on bone regeneration and dental implant osseointegration, an experimental alveolar bone osteotomy rat model was adopted. One month after extraction of maxillary right first molars, osteotomy defects were created at the coronal aspect of each of the extraction sites, and 1×2-mm custom titanium implants were installed into the osteotomies. Coincident with implant placement, Scl-Ab was administered subcutaneously at a dose of 25 mg/kg twice weekly for 10–28 days and compared with a vehicle control. Animals were sacrificed 10, 14, and 28 days after surgery, and maxillae were harvested and analyzed by microcomputed tomography (microCT), histology, and histomorphometry.
Results: microCT analysis demonstrated that the maxillary bone volume fraction was approximately 2- to 2.5-fold greater in Scl-Ab-treated animals compared with vehicle alone at days 14 and 28. Consistent with those findings, two-dimensional bone fill percentages within the coronal osteotomy sites were highest in Scl-Ab treatment groups at 28 days. In addition, bone-implant contact at 28 days was approximately twofold greater in the Scl-Ab group compared with the vehicle control.
Conclusions: These results indicate that systemic Scl-Ab administration enhances osseointegration and bone regeneration around dental implants. This approach offers potential as a treatment modality for patients with low bone mass or bone defects to achieve more predictable bone regeneration at alveolar bone defects and to enhance dental implant osseointegration.

Keywords: dental implants, osseointegration, bone anabolics, sclerostin, bone repair, osseous healing

Introduction

Given the 95.5–98.8% survival and success rates of dental implant reconstructions,[1,2] dental implants have become a predictable treatment option for replacement of missing teeth as a consequence of congenital tooth agenesis, periodontal diseases, or injury. Data provided by the American Academy of Implant Dentistry show that 3 million Americans have dental implant restorations, and the number is growing by 500,000 each year.[3] The estimated US and European markets for dental implants are expected to reach $4.2 billion by 2022.[3] A major clinical challenge for dental implant therapy is improving and accelerating osseointegration of implants to facilitate earlier functional loading. There are two major methods to enhance osseointegration formation around dental implants: implant surface modifications and the use of bone anabolics or antiresorptive agents.[4,5] Some of these approaches have demonstrated favorable improvements;

[1]Department of Periodontics and Oral Medicine, School of Dentistry, University of Michigan, Ann Arbor, Michigan.
[2]Department of Oral- and Craniomaxillofacial Surgery, Faculty of Medicine, Medical Center—University of Freiburg, Freiburg, Germany.
[3]Amgen, Inc., Thousand Oaks, California.
[4]Department of Biomedical Engineering, College of Engineering, University of Michigan College of Engineering, Ann Arbor, Michigan.
[5]Department of Cariology, Restorative Sciences, and Endodontics, School of Dentistry, University of Michigan, Ann Arbor, Michigan.
[6]Phylon Pharma Services, Newbury Park, California.

however, not all are predictable for the myriad bone density issues afflicting edentulous patients,[6] and some antiresorptive agents pose the potential risk of treatment-related osteonecrosis of the jaw.[7] Hence, studies have been conducted to find new potential bone anabolic agents that promote bone regeneration. For instance, a specific inhibitor of cathepsin-K, the enzyme that degrades bone collagen type I, reduces bone resorption; and neutralizing antibodies against sclerostin can stimulate bone formation and decrease bone resorption.[8]

Sclerostin, a 213-amino acid glycoprotein expressed primarily by osteocytes, is a key messenger in communications between osteocytes and osteoblasts and impedes osteoblast differentiation and negatively regulates bone formation.[9,10] Human genetic studies show that patients with loss-of-function mutations in the *SOST* gene that encodes sclerostin have high bone mass and density, with effects on the skull, mandible, ribs, clavicles, and all long bones.[11–13] Animal experiments on *SOST*-null mice have shown increased bone formation, bone mass, and bone strength,[14] while overexpression of the *SOST* gene in mice results in osteopenia.[15] Given the evidence that sclerostin inhibits bone formation, the sclerostin-neutralizing antibody (Scl-Ab) has been developed and investigated for bone disorders in preclinical animal models and human clinical trials. Systemic administration of Scl-Ab to female rats with osteopenia due to ovariectomy-induced estrogen deficiency, or to aged (16-month-old) male rats, was shown to increase bone formation at various bone sites and improve bone mass, mineral apposition rate, and bone strength.[16–18] Moreover, Scl-Ab had potent anabolic effects in bone defect and fracture healing models. Administration of Scl-Ab enhanced new bone formation and bridging at the fracture callus in rats with a 6-mm critical-sized segmental defect in their femoral bone,[19] and our group showed that subcutaneous administration of Scl-Ab for 6 weeks increased the bone volume fraction (BVF), tissue mineral density (TMD), and height of alveolar bone surrounding the molar teeth of rats with experimental periodontitis.[20] Furthermore, net effects of Scl-Ab administration were shown to inhibit bone resorption.[21] Human clinical trials have demonstrated that administration of Scl-Ab to healthy men and postmenopausal women increased bone formation markers and bone mineral density (BMD).[22–26] Such evidence indicates that sclerostin inhibition may be a viable bone anabolic agent to treat bone disorders by increasing bone volume and bone density. Therefore, we hypothesize that the sclerostin-neutralizing antibody as a bone anabolic agent can enhance dental implant osseointegration. Our aim was to investigate the effects of systemic administration of Scl-Ab on dental implant osseointegration in a rat experimental alveolar ridge bone defect model. Bone regeneration and osseointegration around dental implants after systemic Scl-Ab administration were analyzed using microcomputed tomography (microCT), histology, and histomorphometry.

Materials and Methods

Preclinical model of alveolar bone defects from tooth extraction

All procedures were approved by the Institutional Animal Care and Use Committee at the University of Michigan. This study complied with *Animal Research: Reporting of In Vivo Experiments* guidelines for preclinical animal studies. Under general anesthesia using ketamine (50 mg/kg) and xylazine (10 mg/kg), right maxillary first molars were extracted from a total of sixty 8-week-old, male Sprague-Dawley rats. After a 1-month period of socket healing without treatments (Fig. 1), a full-thickness flap was elevated, and a well-type osteotomy defect was created at the extraction site using a customized step drill with sterile saline irrigation. Care was taken to limit perforation of the maxillary sinus floor as the proximity of the limited bone height is such that perforation occasionally occurs during osteotomy preparation. This customized step drill created a defect with a 0.95-mm diameter at the apical 1-mm level and 2.2-mm diameter at the coronal 1-mm level.[27,28] Custom-fabricated, sterile, commercially pure, solid-cylinder titanium implants with a titanium plasma-sprayed surface were used (Institut Straumann AG, Waldenburg, Switzerland). Following preparation of osteotomies, these 1×2-mm titanium implants were press-fit into the osteotomies, ensuring that primary stability was achieved. The coronal end of the implant remained exposed

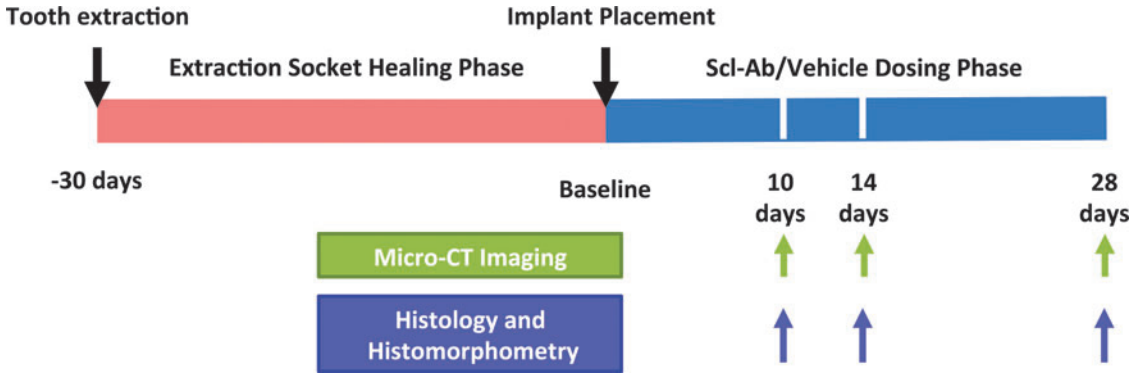

FIG. 1. Study design and time line. Implant surgery was performed 30 days after *right* maxillary first molar extraction. Following wound healing, osteotomies were created and titanium implants were placed concurrent with the initiation of twice-weekly systemic Scl-Ab administration. 3D evaluations (microCT imaging), histology, and histomorphometric measurements were performed at days 10, 14, and 28 after implant installation. 3D, three-dimensional; microCT, microcomputed tomography; Scl-Ab, sclerostin-neutralizing antibody.

approximately 1 mm above the floor of the 2.2-mm diameter step drill defect and the coronal portions of the osseous defects received injectable collagen gel (2.6% bovine type I collagen gel; Tissue Repair Company, San Diego, CA). The flap was approximated and closed with tissue glue (PeriAcryl, n-Butyl Cyanoacrylate; GluStitch Inc., Delta, B.C., Canada). Surgical procedures are illustrated in Figure 2 and a diagram showing the defect and implant position from a lateral projection is presented in Supplementary Figure S1 (Supplementary Data are available online at www.liebertpub.com/tea).

The animals were randomly divided into the Scl-Ab group or vehicle control group, designated to be sacrificed at 10, 14, or 28 days after implant placement (Fig. 1). Subcutaneous Scl-Ab administration at the dose of 25 mg/kg started on the day of surgery and was continued twice per week during the dosing phase of 10, 14, and 28 days.[20] Administration of phosphate-buffered saline (PBS) served as vehicle control. Scl-Ab- and vehicle-treated groups ($n = 5–8$/group) were sacrificed 10, 14, and 28 days after Scl-Ab or vehicle administration and their maxillae were harvested and evaluated by microCT, histology, and histomorphometry.

Maxilla harvest, microCT, and histological preparation and analysis

The animals were euthanized by carbon dioxide inhalation overdose at designated time points and maxillary specimens were harvested and fixed in 10% neutral-buffered formalin for 2 days. The specimens were then transferred to 70% alcohol for microCT scanning. Each group and time point initiated with $n = 10–12$ animals/implants. Due to surgical complications, early implant loss, or histological processing, the total number of specimens available for evaluation reduced to a total of 5–8 animals per group available for final analysis and did not relate to the treatment rendered.

Maxillary specimens were scanned using a cone-beam microCT system (GE HealthCare BioSciences, Model Pxs5-928EA; GE Healthcare, London, ON, Canada), following settings as previously described.[20] Scans were reconstructed and two- and three-dimensional (3D) images were generated for all specimens. We followed methods previously described[20] and modified the measurements of BVF and TMD using GEMS MicroView software (eXplore MicroView v.2.1.2, Analysis Plus; GE Healthcare). BVF indicates the 3D measurement of bone formation (bone quantity), while TMD indicates the 3D measurement of the quality of newly formed bone (bone quality).

After microCT scanning, specimens were dehydrated in step gradients of alcohol, infiltrated, and embedded in methyl methacrylate by routine histological methods. One sagittal section of approximately 50-μm thickness was cut along each implant's long axis using a diamond saw at the central portion of each implant (Well Diamond Wire Saws, Inc., Norcross, GA). Each specimen was attached to a plastic slide, ground to ~25 μm with an EXAKT Micro Grinder 400 (Exakt Medical Instruments, Inc., Oklahoma City, OK), and polished to an optical finish. The sections were placed in pH 4 hydrochloric acid solution for 15 s, rinsed three times for 1 min with distilled water, stained with 0.2% methylene blue for 1 min, rinsed three times for 1 min with PBS, stained with 0.2% basic fuchsin for 1 min, rinsed with distilled water thoroughly, and dried. After histological preparation, slides were coded and examined by two examiners blinded to treatment group allocation (S.H.Y. and T.F.).

Histological analysis was used to evaluate the spatial and temporal sequences of osteogenesis and bone-implant contact (BIC) during oral implant osseointegration. Histomorphometric analyses were performed using a Nikon Eclipse 50i microscope (Nikon Instruments, Inc., Melville, NY) fitted with a DS-5M digital color camera and NIS-Elements software (Nikon Instruments, Inc.). Standard parameters of

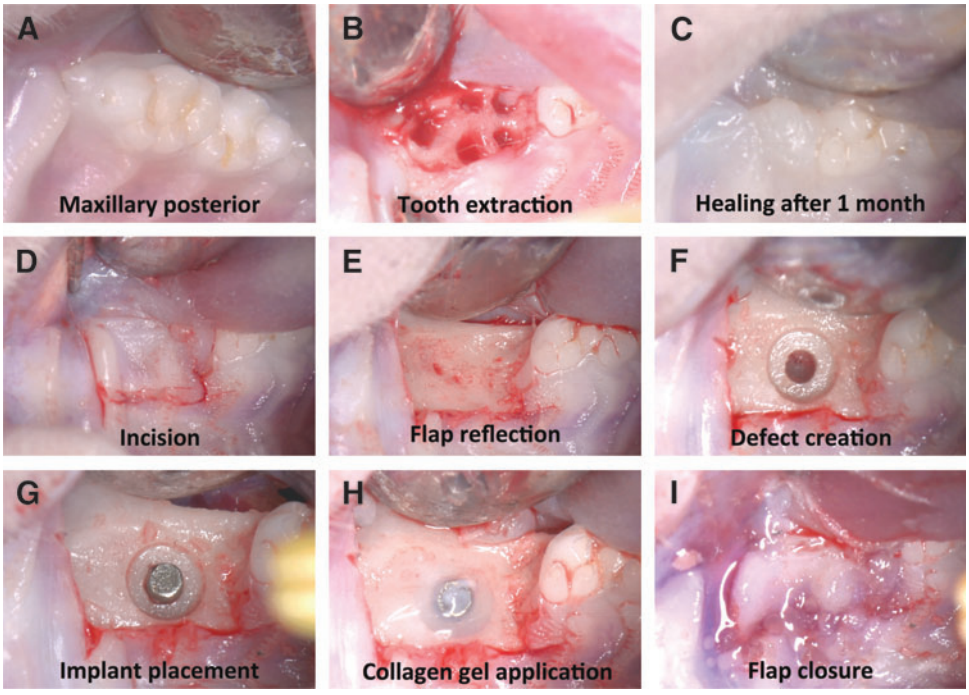

FIG. 2. Surgical procedures of maxillary molar extraction and implant placement. **(A)** Occlusal (*top*) view of maxillary *right* molars. **(B)** Socket after first molar extraction. **(C)** Socket wound healing 1 month after extraction. **(D)** Gingival flap design. **(E)** Flap reflection and alveolar ridge exposure. **(F)** Osteotomy created by a customized step drill. **(G)** Placement of the titanium implant into the osteotomy defect. **(H)** Application of collagen gel around the titanium implant. **(I)** Closure of the wound with tissue glue.

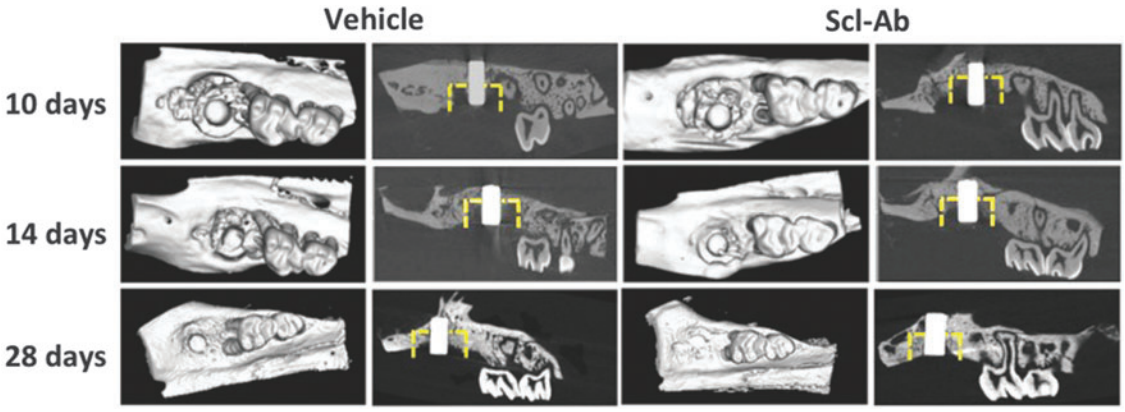

FIG. 3. microCT images. Representative microCT images of maxillary alveolar bone surrounding the titanium implants at days 10, 14, and 28 after placement of dental implants. The *yellow dotted line* marks the approximate dimensions of the defect. Two-dimensional sagittal images and 3D images of maxillae show visual differences in bone formation around the dental implants between the Scl-Ab-treated group and the vehicle group.

osteogenesis and osseointegration were measured and analyzed as previously described for the percentage of bone fill and BIC.[27]

Statistical analyses

Data for all measurements on each parameter from microCT and histomorphometry were analyzed and compared using Prism 7 software (GraphPad Software, Inc., La Jolla, CA). Comparisons among multiple groups were performed with one-way analysis of variance, while comparisons between two groups were done with Student's *t*-test.

Results

microCT analysis

As shown in Figure 3, minimal amounts of newly formed bone were found at day 10 in both the Scl-Ab and vehicle groups. By day 14, greater evidence of osteogenesis was seen in the defects of the Scl-Ab group when compared with vehicle-treated animals. Bone appeared to form from the alveolar wall of surgically created osteotomies, along with limited new bone formation along the surfaces of dental implants at days 10 and 14. By day 28, greater amounts of new bone were seen in the defects of the Scl-Ab group compared with vehicle controls. Importantly, new bone had formed on implant surfaces of the vehicle and Scl-Ab groups at day 28, with more such bone evident in the Scl-Ab group, suggesting better osseointegration and greater BIC. Moreover, newly formed bone can be recognized due to the different grayscale levels between new and old bone at days 10 and 14. Such differences in grayscale levels from microCT images of new and old bone in 28-day specimens were less distinguishable, indicating that the density of newly formed bone increased over time. We also found that new bone formation in the coronal portion of defects showed some variability. Consistent with microCT imaging observations, 3D microCT measurements showed that BVF in the Scl-Ab group was approximately twofold greater than that in the control group at day 14 and 2.5 times greater in Scl-Ab sites than vehicle-treated sites

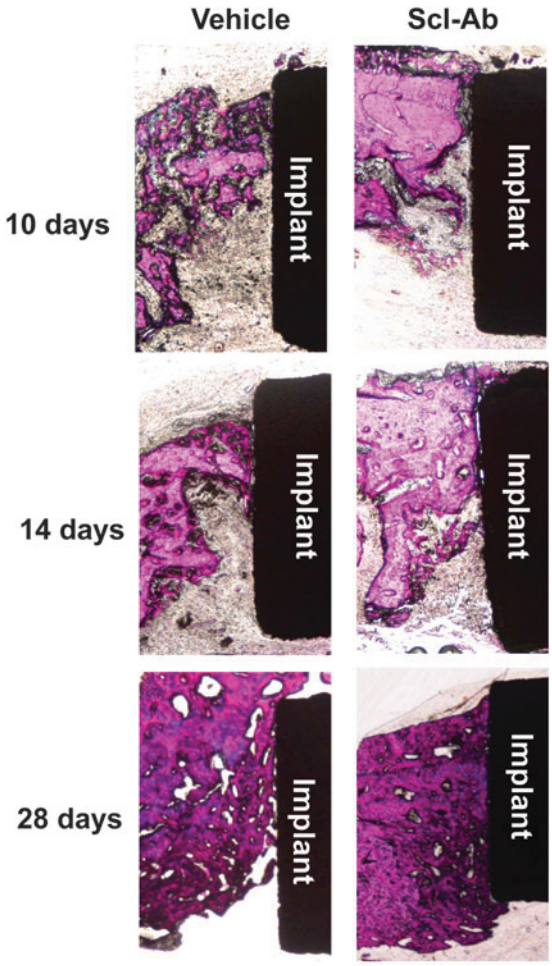

FIG. 4. Histology of resin-embedded sections of specimens with methylene *blue* and basic fuchsin staining. New bone formation was found in all the defects. Over time, osseointegration was also observed. Greater bone formation was seen in the Scl-Ab group compared with the phosphate-buffered saline vehicle group at days 14 and 28.

at day 28 (Fig. 5A). There were no differences in TMD among groups (Fig. 5B).

Histology and histomorphometry

At days 10 and 14, there was minimal new bone formation (observed histologically) on defect walls in both groups as it was more difficult to identify newly formed bone on surfaces of dental implants at the early time points (Fig. 4) compared with microCT image analysis. The greatest amount of bone formation was observed at 28 days, most notably in the Scl-Ab group, by assessing the physical appearance of woven bone formation within the osseous defects. Osseointegration was visible on the surface of dental implants in both groups at 28 days. Similar to these qualitative histological observations, histomorphometry did not display statistically significant differences between the two groups for bone fill or BIC at days 10 and 14 (Fig. 5C, D). However, at day 28, bone fill and BIC were significantly greater in the Scl-Ab group compared with controls, indicating that Scl-Ab stimulated greater osseous regeneration and osseointegration compared with controls.

Discussion

In this study, we utilized a well-type alveolar bone osteotomy model to investigate the effects of systemically administered Scl-Ab on bone regeneration and osseointegration around dental implants. The data showed that Scl-Ab not only improved bone formation around implants but also enhanced osseointegration between the bone and implant.

This rat dental implant model has been developed and well characterized by our group.[27–29] We have investigated the bone wound healing process of this rat osteotomy model and discovered four phases of wound healing over time, as previously described: an inflammation phase 1–3 days after surgery; a proliferation and granulation phase during days 4–

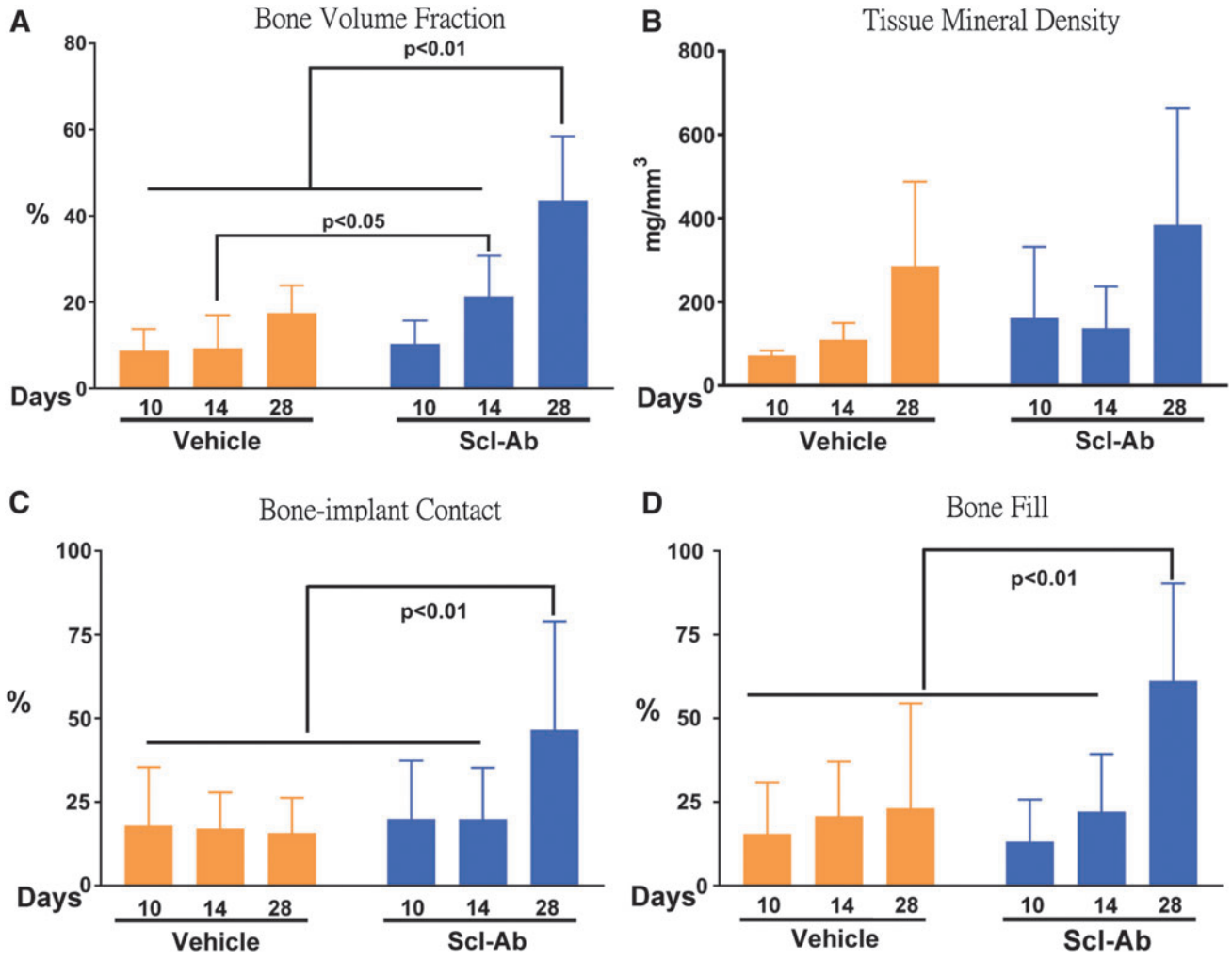

FIG. 5. microCT assessments of BVF and TMD and histomorphometry measurements of BVF and BIC. **(A)** At day 14, the Scl-Ab group had more BVF than the vehicle group by *t*-test analysis ($p < 0.05$). Furthermore, the Scl-Ab group at day 28 presented the largest BVF through one-way ANOVA. **(B)** Assessment of TMD indicated no difference between Scl-Ab and vehicle groups. **(C, D)** The Scl-Ab group had the statistically greatest BIC and bone fill percentage at day 28 compared with the vehicle group, as analyzed by one-way ANOVA. ANOVA, analysis of variance; BVF, bone volume fraction; BIC, bone-implant contact; TMD, tissue mineral density.

7, an initial bone formation phase from day 10 to 14, and a continuous osteogenic phase during days 21–28. In addition, we have validated this model by exploring the effects of locally applied growth factors on bone formation around dental mini-implants and osseointegration between bone and dental implant surfaces.[27,28] While we did not perform specific biomechanical testing in this study, we noted that BIC, BVF, TMD, and BMD have strong and moderately strong correlation with the functional apparent modulus, which indicates that histology and microCT data are parallel with mechanical test data, as we have previously reported.[27,30,31] Based on this model, we chose the experimental approach and time points of 10, 14, and 28 days to study effects of the sclerostin antibody on bone formation and dental implant osseointegration.

Osseointegration is a critical factor for dental implant function and survival, which depends on adequate amounts of bone formed around the dental implant (bone volume-wise) and adequate contact between the dental implant and surrounding alveolar bone (osseointegration).[32]

Sclerostin is a monomeric glycoprotein produced by osteocytes, which binds to LRP5/6 coreceptors on the cell surface of osteoblast lineage cells to inhibit the osteogenic Wnt signaling pathway.[33] The Wnt signaling pathway has a well-documented effect on embryonic skeleton development, bone modeling, postnatal bone formation, and bone homeostasis.[34] In the present study, microCT analysis showed that BVF at day 14 (the initial bone formation phase) was greater in the Scl-Ab group versus the control group. There are several possible mechanisms for this result: first, the Wnt signaling pathway participates in vascularization.[35,36] Due to blockade of sclerostin's actions by Scl-Ab, vascularization in the defects appeared to be improved. As a result, more bone formation occurred in the Scl-Ab group. Second, because the Wnt signaling pathway has been shown to increase mesenchymal stem cell migration and proliferation,[37–39] Scl-Ab treatment may induce greater numbers of mesenchymal stem cells to migrate to the wound site and proliferate, which may result in more bone formation at early time points. Third, evidence showed that Wnt improves osteoblast differentiation.[40–42] Therefore, more osteoblasts may be formed in the Scl-Ab group, which produced more bone in the defect. From microCT sagittal image analysis, we observed that the newly formed bone in the defect was not evenly distributed for both Scl-Ab and control groups, which may explain why the BVF data from microCT analysis did not mirror the bone fill percentage measured from histology sections at day 14. At day 28, more bone formation was seen in both groups compared with days 10 and 14, with greater bone formation in the Scl-Ab group at day 28 than the control group. Sclerostin is a key factor that affects bone modeling and remodeling. Blocking sclerostin results in not only increased bone formation but also decreased bone resorption.[21,43] At the later time point of 28 days, we consider that effects of sclerostin on bone remodeling (the net functions of anabolic and catabolic actions) may have a more significant impact than purely bone formation (bone anabolic action) in Scl-Ab-treated defects, although Scl-Ab antiresorptive effects started to be present at day 14 based on BVF results. On the other hand, we did not note differences in TMD between the two groups, which needs further investigation in the future given that there is not always a strong correlation between TMD and BVF.[30,31]

In this study, there was limited bone formation on the surface of dental implants at days 10 and 14 for both groups, yet obvious bone formation was observed on the surface of implants by day 28. Histomorphometric results showed that the Scl-Ab group at day 28 had the greatest BIC, which is consistent with the interpretation that Scl-Ab increased osseointegration. One limitation of the current study is that we have not determined the extent to which enhanced osseointegration with Scl-Ab was the result of increased bone formation (an anabolic effect) or decreased bone resorption (an anticatabolic effect). Future studies using fluorochrome labeling of newly formed bone may provide such insights.

In the present study, systemic Scl-Ab administration increased bone regeneration in a well-type alveolar bone defect and also enhanced osseointegration of dental implants, as shown by increased BIC. Future directions using this approach include the consideration of local delivery of Scl-Ab around dental implants to promote a more targeted delivery. Our current results also support future clinical studies to investigate the effects of Scl-Ab in promoting alveolar bone regeneration and early osseointegration in patients requiring dental implants to reconstruct edentulous areas.

Acknowledgments

The authors thank Hua Z. Ke, Mike Ominsky, and James Sugai for their assistance with this investigation. This study was supported by the Osteology Foundation (14-040, Q.J.), the Delta Dental Foundation (S.H.Y.), and NIH U24 DE026915-02 (W.V.G.). This work was supported by a research fellowship to T.F. by the Osteology Foundation, Lucerne, Switzerland. The authors appreciate the provision of dental implants from Institut Straumann and sclerostin-neutralizing antibody from Amgen.

Disclosure Statement

No competing financial interests exist.

References

1. Buser, D., Janner, S.F., Wittneben, J.G., Brägger, U., Ramseier, C.A., and Salvi, G.E. 10-year survival and success rates of 511 titanium implants with a sandblasted and acid-etched surface: a retrospective study in 303 partially edentulous patients. Clin Implant Dent Relat Res **14,** 839, 2012.
2. Wittneben, J.G., Buser, D., Salvi, G.E., Bürgin, W., Hicklin, S., and Brägger, U. Complication and failure rates with implant-supported fixed dental prostheses and single crowns: a 10-year retrospective study. Clin Implant Dent Relat Res **16,** 356, 2014.
3. Mohan, S., and Baylink, D.J. Evidence that the inhibition of TE85 human bone cell proliferation by agents which stimulate cAMP production may in part be mediated by changes in the IGF-II regulatory system. Growth Regul **1,** 110, 1991.

4. Le Guéhennec, L., Soueidan, A., Layrolle, P., and Amouriq, Y. Surface treatments of titanium dental implants for rapid osseointegration. Dent Mater **23,** 844, 2007.
5. Gabet, Y., Müller, R., Levy, J., *et al.* Parathyroid hormone 1–34 enhances titanium implant anchorage in low-density trabecular bone: a correlative micro-computed tomographic and biomechanical analysis. Bone **39,** 276, 2006.
6. Barfeie, A., Wilson, J., and Rees, J. Implant surface characteristics and their effect on osseointegration. Br Dent J **218,** E9, 2015.
7. Vohra, F., Al-Rifaiy, M.Q., Almas, K., and Javed, F. Efficacy of systemic bisphosphonate delivery on osseointegration of implants under osteoporotic conditions: lessons from animal studies. Arch Oral Biol **59,** 912, 2014.
8. Saag, K.G., Petersen, J., Brandi, M.L., *et al.* Romosozumab or alendronate for fracture prevention in women with osteoporosis. N Engl J Med **377,** 1417, 2017.
9. ten Dijke, P., Krause, C., de Gorter, D.J., Lowik, C.W., and van Bezooijen, R.L. Osteocyte-derived sclerostin inhibits bone formation: its role in bone morphogenetic protein and Wnt signaling. J Bone Joint Surg Am **90**(Suppl. 1), 31, 2008.
10. van Bezooijen, R.L., Roelen, B.A., Visser, A., *et al.* Sclerostin is an osteocyte-expressed negative regulator of bone formation, but not a classical BMP antagonist. J Exp Med **199,** 805, 2004.
11. Balemans, W., Cleiren, E., Siebers, U., Horst, J., and Van Hul, W. A generalized skeletal hyperostosis in two siblings caused by a novel mutation in the SOST gene. Bone **36,** 943, 2005.
12. Balemans, W., Ebeling, M., Patel, N., *et al.* Increased bone density in sclerosteosis is due to the deficiency of a novel secreted protein (SOST). Hum Mol Genet **10,** 537, 2001.
13. Brunkow, M.E., Gardner, J.C., Van Ness, J., *et al.* Bone dysplasia sclerosteosis results from loss of the SOST gene product, a novel cystine knot-containing protein. Am J Hum Genet **68,** 577, 2001.
14. Li, X., Ominsky, M.S., Niu, Q.T., *et al.* Targeted deletion of the sclerostin gene in mice results in increased bone formation and bone strength. J Bone Miner Res **23,** 860, 2008.
15. Loots, G.G., Kneissel, M., Keller, H., *et al.* Genomic deletion of a long-range bone enhancer misregulates sclerostin in Van Buchem disease. Genome Res **15,** 928, 2005.
16. Li, X., Ominsky, M.S., Warmington, K.S., *et al.* Sclerostin antibody treatment increases bone formation, bone mass, and bone strength in a rat model of postmenopausal osteoporosis. J Bone Miner Res **24,** 578, 2009.
17. Li, X., Ominsky, M.S., Warmington, K.S., *et al.* Increased bone formation and bone mass induced by sclerostin antibody is not affected by pretreatment or cotreatment with alendronate in osteopenic, ovariectomized rats. Endocrinology **152,** 3312, 2011.
18. Li, X., Warmington, K.S., Niu, Q.T., *et al.* Inhibition of sclerostin by monoclonal antibody increases bone formation, bone mass, and bone strength in aged male rats. J Bone Miner Res **25,** 2647, 2010.
19. Virk, M.S., Alaee, F., Tang, H., Ominsky, M.S., Ke, H.Z., and Lieberman, J.R. Systemic administration of sclerostin antibody enhances bone repair in a critical-sized femoral defect in a rat model. J Bone Joint Surg Am **95,** 694, 2013.
20. Taut, A.D., Jin, Q., Chung, J.H., *et al.* Sclerostin antibody stimulates bone regeneration after experimental periodontitis. J Bone Miner Res **28,** 2347, 2013.
21. Stolina, M., Dwyer, D., Niu, Q.T., *et al.* Temporal changes in systemic and local expression of bone turnover markers during six months of sclerostin antibody administration to ovariectomized rats. Bone **67,** 305, 2014.
22. Becker, C.B. Sclerostin inhibition for osteoporosis—a new approach. N Engl J Med **370,** 476, 2014.
23. McColm, J., Hu, L., Womack, T., Tang, C.C., and Chiang, A.Y. Single- and multiple-dose randomized studies of blosozumab, a monoclonal antibody against sclerostin, in healthy postmenopausal women. J Bone Miner Res **29,** 935, 2014.
24. Mirza, F.S., Padhi, I.D., Raisz, L.G., and Lorenzo, J.A. Serum sclerostin levels negatively correlate with parathyroid hormone levels and free estrogen index in postmenopausal women. J Clin Endocrinol Metab **95,** 1991, 2010.
25. Padhi, D., Allison, M., Kivitz, A.J., *et al.* Multiple doses of sclerostin antibody romosozumab in healthy men and postmenopausal women with low bone mass: a randomized, double-blind, placebo-controlled study. J Clin Pharmacol **23,** 239, 2013.
26. Padhi, D., Jang, G., Stouch, B., Fang, L., and Posvar, E. Single-dose, placebo-controlled, randomized study of AMG 785, a sclerostin monoclonal antibody. J Bone Miner Res **26,** 19, 2011.
27. Chang, P.C., Seol, Y.J., Cirelli, J.A., *et al.* PDGF-B gene therapy accelerates bone engineering and oral implant osseointegration. Gene Ther **17,** 95, 2010.
28. Dunn, C.A., Jin, Q., Taba, M., Jr., Franceschi, R.T., Bruce Rutherford, R., and Giannobile, W.V. BMP gene delivery for alveolar bone engineering at dental implant defects. Mol Ther **11,** 294, 2005.
29. Lin, Z., Rios, H.F., Volk, S.L., Sugai, J.V., Jin, Q., and Giannobile, W.V. Gene expression dynamics during bone healing and osseointegration. J Periodontol **82,** 1007, 2011.
30. Chang, P.C., Lang, N.P., and Giannobile, W.V. Evaluation of functional dynamics during osseointegration and regeneration associated with oral implants. Clin Oral Implants Res **21,** 1, 2010.
31. Chang, P.C., Seol, Y.J., Goldstein, S.A., and Giannobile, W.V. Determination of the dynamics of healing at the tissue-implant interface by means of microcomputed tomography and functional apparent moduli. Int J Oral Maxillofac Implants **28,** 68, 2013.
32. Branemark, P.I., Hansson, B.O., Adell, R., *et al.* Osseointegrated implants in the treatment of the edentulous jaw. Experience from a 10-year period. Scand J Plast Reconstr Surg Suppl **16,** 1, 1977.
33. Li, X., Zhang, Y., Kang, H., *et al.* Sclerostin binds to LRP5/6 and antagonizes canonical Wnt signaling. J Biol Chem **280,** 19883, 2005.
34. Maupin, K.A., Droscha, C.J., and Williams, B.O. A comprehensive overview of skeletal phenotypes associated with alterations in Wnt/beta-catenin signaling in humans and mice. Bone Res **1,** 27, 2013.
35. Barbacena, P., Carvalho, J.R., and Franco, C.A. Endothelial cell dynamics in vascular remodelling. Clin Hemorheol Microcirc **64,** 557, 2016.
36. Korn, C., and Augustin, H.G. Mechanisms of vessel pruning and regression. Dev Cell **34,** 5, 2015.
37. He, J., Meng, G., Yao, R., Jiang, B., Wu, Y., and Wu, F. The essential role of inorganic substrate in the migration

and osteoblastic differentiation of mesenchymal stem cells. J Mech Behav Biomed Mater **59,** 353, 2016.
38. Boland, G.M., Perkins, G., Hall, D.J., and Tuan, R.S. Wnt 3a promotes proliferation and suppresses osteogenic differentiation of adult human mesenchymal stem cells. J Cell Biochem **93,** 1210, 2004.
39. Etheridge, S.L., Spencer, G.J., Heath, D.J., and Genever, P.G. Expression profiling and functional analysis of wnt signaling mechanisms in mesenchymal stem cells. Stem Cells **22,** 849, 2004.
40. Krause, C., Korchynskyi, O., de Rooij, K., *et al.* Distinct modes of inhibition by sclerostin on bone morphogenetic protein and Wnt signaling pathways. J Biol Chem **285,** 41614, 2010.
41. Olivares-Navarrete, R., Hyzy, S.L., Park, J.H., *et al.* Mediation of osteogenic differentiation of human mesenchymal stem cells on titanium surfaces by a Wnt-integrin feedback loop. Biomaterials **32,** 6399, 2011.
42. Krishnan, V., Bryant, H.U., and Macdougald, O.A. Regulation of bone mass by Wnt signaling. J Clin Invest **116,** 1202, 2006.
43. Houben, A., Kostanova-Poliakova, D., Weissenbock, M., *et al.* beta-catenin activity in late hypertrophic chondrocytes locally orchestrates osteoblastogenesis and osteoclastogenesis. Development **143,** 3826, 2016.

Address correspondence to:
William V. Giannobile, DDS, DMedSc
Department of Periodontics and Oral Medicine
School of Dentistry
University of Michigan
1011 N. University Ave.
Ann Arbor, MI 48109-1078

E-mail: wgiannob@umich.edu

Qiming Jin, DDS, MS, PhD
Department of Cariology, Restorative Sciences and Endodontics
School of Dentistry
University of Michigan,
1011 N. University Ave.
Ann Arbor, MI 48109-1078

E-mail: jinqm@umich.edu

Received: January 18, 2018
Accepted: May 15, 2018
Online Publication Date: August 27, 2018